Current Trends in
Fashion Technology & Textile Engineering
ISSN: 2577-2929

Juniper Publishers
key to the Researchers

Research Article
Volume 8 Issue 3- April 2023
DOI: 10.19080/CTFTTE.2023.08.555737

Curr Trends Fashion Technol Textile Eng
Copyright © All rights are reserved by George Patermarakis

Mechanism of C.I. Reactive Red 120 Uptake from Solution by Anodic Alumina Films

George Patermarakis[1]* and Alexandros A Vassiliadis[2]

[1]*Department of Biomedical Engineering, University of West Attica, Greece*

[2]*Dyeing, Finishing, Dyestuffs and Advanced Polymers Laboratory, University of West Attica, Greece*

Submission: March 13, 2023; **Published:** April 14, 2023

***Corresponding author:** George Patermarakis, Department of Biomedical Engineering, University of West Attica, Greece

Abstract

The uptake by mesoporous anodic alumina films of C.I. Reactive Red 120 from its solution was studied to be assessed as a method effective to remove azo-reactive dyes from industrial effluents and the uptake mechanism was revealed. The alumina was used after its deactivation as a destructive and its activation as an adsorptive agent. It was found that the process is slow, and a quasi-equilibrium is finally setup. The results suggest that the mechanism of dye removal from solution embraces a mixed physical and chemical adsorption of large dye anions where the negative charge is at least partially compensated by protons adsorbed on basic surface sites so that an about monomolecular dye layer is formed while the pH of solution increases. Above this layer a multimolecular dye layer grows by physical adsorption and flocculation/coagulation. After prolonged drying of the adsorbent/deposited dye layer system, this layer is easily mechanically removed as flakes and both adsorbent and dye are recovered. The method can be variously improved to optimize the rate of dye removal from solution and the final amount of dye taken up, as well as to further facilitate the separation of the dye and the adsorbent.

Keywords: C.I. Reactive Red 120; Anodic alumina adsorbent; Dyeing; Physical–chemical adsorption; Flocculation; Coagulation

Introduction

It is well known that the discharge of industrial effluents containing textile-dye residuals, mainly into water-bodies recipients and secondly in soil ones, is the origin of many serious environmental and health problems. These effluents are generally toxic and carcinogenic. The contained dyes have a complex structure, mainly based on aromatic amines the partial degradation of which also generates various toxic by-products. The wastewater resulting from textile dyeing processes is very difficult to treat by the conventional activated sludge systems. Due to the non-biodegradable nature of the dyes, these in wastewater remain unaffected. To remove the dyes, many different physicochemical methods, such as coagulation/flocculation, adsorption on clay, perlite, activated carbon, carbon composites and biomaterials (e.g., algae, fungi, agricultural products and by-products), and other techniques, such as the reverse osmosis, were developed [1-3].

By these methods the contaminants, dyes and dye by-products, are actually transferred from one phase to another only, or these are densified in the initial phase, thus the problem remains essentially unsolved [4-9]. Recovery of dyes by such methods may further require their degradation and total mineralization to simple molecules as H_2O, CO_2, N_2, complicating the entire effluent processing practice. At a first glance, the best solution seems to be the destruction of dye molecules and dye by-products and their mineralization within the effluents, on which research is thus also focused.

Such methods are the advanced oxidation processes (AOPs), that is the ozonation and other combined methods including ultra-violet (UV) radiation, H_2O_2 and O_3 (UV/H_2O_2, $UV/O_3/H_2O_2$), which can cause the destruction of chromophore group in dye molecule and, thus, the discoloration of textile effluent. In the specific case of azo-reactive textile dyes the azo double bond –N=N– breaks initially, then intermediate colorless products are formed, e.g., nitrosamines. These products can be further degraded until their complete mineralization [10-13]. Methods combining O_3 with other treatment techniques such as radiofrequency alternating electric field (RFAEF), ultra-sound (US), UV and H_2O_2 ($RFAEF/O_3$, US/O_3, $US/O_3/UV$, $US/O_3/H_2O_2$) have also displayed important synergetic effects and generally promising results [1,14-16]. As the AOPs, various other pulsed power treatment techniques that generate

in situ highly strong oxidizing agents such as OH•, H•, O•, H_2O_2, O_2 and O_3 have also been successfully tested recently in reactive azo-dye effluents [17-20]. AOPs also include electrochemical methods that produce active species as above.

Additional mixed methods were also tried such as sono-electrocoagulation including sono-activation together with electrochemical treatment, adsorption and coagulation/flocculation [21]. A large amount of work has been done on the removal and destruction of dyes which implies that the problem persists to remain basically unsolved and the related research issue is still open. The detailed mechanisms of the destruction of chromophore groups and of the entire dye molecules up to their mineralization, in terms of the specific behavior of each separate ring, functional group, atom and substituent and of the related elementary processes, is very complex. This complexity is much more enhanced when the different active species formed during, e.g., an electrochemical process, is also considered. As an example, when H_2O_2 and O_3 are involved, these produce many other species/radicals.

Considering, e.g., O_3, it reacts with H_2O ($O_3 + H_2O \rightarrow HO_3^+ + OH^-$, $HO_3^+ + OH^- \rightarrow 2HO_2•$, $O_3 + HO_2• \rightarrow HO• + 2O_2$) [22], and generally takes part in numerous processes where many active species and radicals are formed while it can also react directly with organic compounds [1]. The oxidative effect of the previous agents is not always clear enough. For example, the OH• and H• do not present only an oxidative behavior [23]; both can abstract H atoms from various organic compounds to form H_2 and H_2O molecules or can be added, e.g., to aromatic rings as a result of their electrophilic character, that of H• being slight and that of OH• more pronounced. Also, they can react with functional groups as a result of their redox properties. Moreover, they react with inorganic compounds. H• behaves generally as a reducing agent, but there are exceptions where it behaves as an oxidizing agent, while the reaction $H• + OH^- \rightarrow e_{aq}^- + H_2O$, where e_{aq}^- is hydrated electron, may be looked upon as an acid–base process [23]. Other active species/radicals also show other complexities. A full elucidation of the mechanisms of all the overall and elementary processes and related kinetics with precise physical meaning are thus unfeasible.

When AOP related methods are applied, the complexity of the elementary processes means also that harmful intermediate compounds (some of which are unknown) are probably formed that are not totally destroyed and, thus, not absent at the end of processing the industrial effluents. To avoid such complexities and dangers, from all the above it is inferred that a method embracing the adsorption of dye from effluents on suitable adsorbents that is followed by an easy recovery (or destruction) of dyes and by the recovery of adsorbent is an attractive ideal method. When dye-containing effluents are disposed into, e.g., water-bodies recipients, light absorption hinders the bio-physicochemical processes that are vital for the eco-system. A method like the above satisfies the first main required result of processing such effluents before disposal, that is the discoloration. Here, the application of such a method is first examined.

Porous anodic alumina film (PAAF) is a highly adsorptive material and effective catalyst or catalyst support for the decomposition and oxidation of organic compounds and pollutant molecules [24-27]. Al anodization in suitable pore forming electrolytes, e.g., oxalic, sulfuric, phosphoric, tartaric, etc. acid, produces PAAFs [28]. PAAFs grow in three sequential stages, the first and second transient stages and the third steady-state stage where their structures become a close-packed array of about hexagonal columnar cells [29-32]. Each cell contains an elongated pore vertical to Al surface, extending from the top surface to near the metal|oxide interface, while a thin spherical sector shell-shaped barrier-type layer with thickness ≈ 1 nm per V of applied voltage exists among the interface and pore bottom [29-32]. While the first two transient stages are short, the third can be desirably short or long. The length (up to many tens μm) and diameter of pores (a few nm up to some tens nm), porosity and real surface of PAAF can be suitably designed.

The uptake of C.I. Reactive Red 120 from solution by PAAF and subsequent dye recovery from PAAF surface are investigated. A new combined method of dye uptake followed by recovery of dye and adsorbent is thus invented.

Materials and Methods

Three of the most representative and commonly applied azo-reactive dyes, most suitable for dyeing cotton and polyester/cotton blends, are C.I. Reactive Yellow 84 (RY 84), C.I. Reactive Red 120 (RR 120) and C.I. Reactive Blue 98 (RB 198). Their molar formula and mass and wavelength of maximum absorbance are $C_{56}H_{38}Cl_2N_{14}Na_6O_{20}S_6$, 1628.22, 400 nm, $C_{44}H_{24}Cl_2N_{14}O_{20}S_6Na_6$, 1469.98, 535 nm, and $C_{41}H_{30}Cl_4N_{14}Na_4O_{14}S_4$, 1404.80, 625 nm, respectively [33]. These dyes are anionic, highly soluble in water. The dye RR 120 has intermediate values of λ_{max}, molar mass, molar formula complexity and size of molecule (thus, of anion) and its structural formula is given in Figure 1 [33]. Solutions of these dyes have been previously processed by the RFAEF/O_3 method [1] and they showed a qualitatively similar behavior, but the mean discoloration rate of RR 120 was ≈ 3 and 2 times faster than that of RY 84 and RB 198. This must be related to its structure, indicating generally a higher reactivity of this dye and most probably a faster uptake of the dye by an adsorbent so that long lasting experiments would be avoided.

Therefore, this dye was chosen for the present study. A solution of RR 120 (Everlight Chemical Industrial Co, Taiwan) with a concentration of 50 mg dm^{-3} (or 3.4014×10^{-5} mol dm^{-3}) having pH 6.75 was used for the experiments.

How to cite this article: Patermarakis G, Vassiliadis AA. Mechanism of C.I. Reactive Red 120 Uptake from Solution by Anodic Alumina Films. Curr Trends Fashion Technol Textile Eng. 2023; 8(3): 555737. DOI: 10.19080/CTFTTE.2023.08.555737

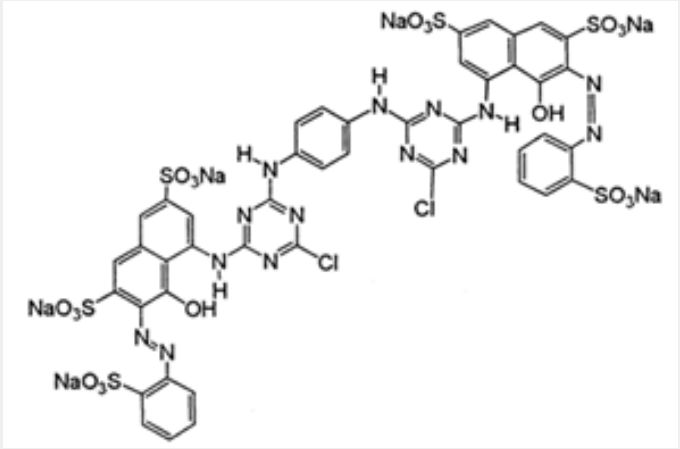

Figure 1: Structure of C.I. Reactive Red 120 (RR 120) dye.

The dissolution of RR 120 molecule gives an anion with charge −6 and 6 Na^+ ions. The dimensions of the chemical molecule were previously calculated using ChemBio 3D ultra-version 12.0, and a representative dimension 2.48 nm, accessible area 14.84 nm^2, molecular area 8.83 nm^3 and solvent excluded volume 0.83 nm^3 were found [2], so the RR 120 molecule and anion are large enough. With the use of a spectrophotometer UV/VIS Hitachi U-1100 and reference plot of absorbance vs. dye concentration, the dye removal efficiency was determined during the experiments.

To form PAAF adsorbents, sheets of Al (purity ≥ 99.9518%, Merck pro-analysis) as anode and Pb (purity ≥ 99.968%, Merck pro-analysis) as cathode, both having a thickness of 0.5 mm, were used. Each Al electrode with dimensions of conductive surface 3 × 3 cm^2 had a stem 5 × 1 cm^2 originating from the center of a side. It was insulated except for its bare upper edge with length 1 cm for the electrical connection. Each Pb electrode with conductive surface 5 × 5 cm^2 also had similarly a stem 3 × 1 cm^2 insulated except of its bare upper edge with length 1 cm. The total conductive geometric surface area (electrochemically active surface) of Al was thus S_g = 18.55 cm^2.

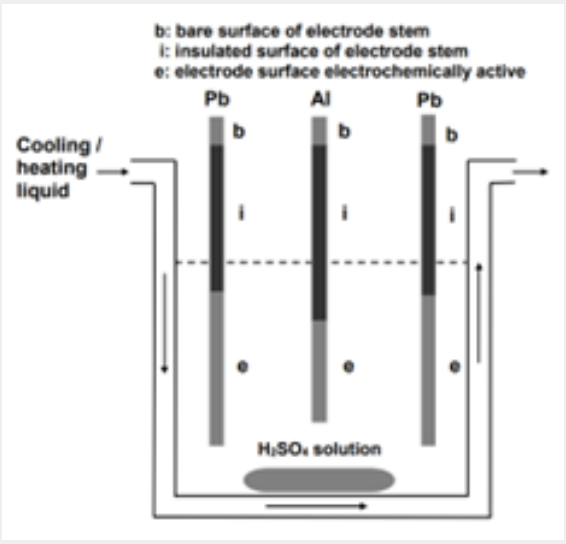

Figure 2: Electrolytic cell setup for Al anodization.

For Al anodization a homemade power supplier (Potentiostat – Automatic Reference Control – Model: PA–495) was used, working either galvanostatically or potentiostatically with upper limits of power output ≈ 50 W, current (I) 2 A and voltage (ΔV) ≈ 35 V. For uniform as possible growth of PAAF, each Al specimen was placed among two Pb electrodes each at 5 cm apart from Al, as shown in Figure 2**.** The anodization of Al was performed in thermostated and vigorously stirred bath solution of H_2SO_4 at

How to cite this article: Patermarakis G, Vassiliadis AA. Mechanism of C.I. Reactive Red 120 Uptake from Solution by Anodic Alumina Films. Curr Trends Fashion Technol Textile Eng. 2023; 8(3): 555737. DOI: 10.19080/CTFTTE.2023.08.555737

concentration 0.51 mol dm^{-3} (5% w/v), temperature (T) = 25 °C, times (t) = 7200 and 2280 s and anodic potential vs. Hg/Hg_2SO_4 reference electrode used (P_{an} vs. ref. el.) = 23 V. Because $P_{ref.el.}$ vs. SHE = 0.615 V [34], then P_{an} vs. SHE (P_{an}) = 23.615 V. At these conditions, several physical and structural features of PAAFs have been previously determined [35], which facilitate the analysis in this work. At these two *t*s the mass of PAAF in each Al specimen is m = 0.6355 and 0.1567 g and the mean film thickness is $h_f \approx$ 183.6 and 32.2 μm.

Results and Discussion

Four Al specimens were anodized at the aforesaid conditions and t = 7200 s (Materials and Methods). In each Al specimen the thickness of PAAF was thus $h_f \approx$ 183.6 μm which approaches the maximum limiting one [35], while the total mass of oxide is 4 × 0.6355 = 2.542 g. The specific real surface of PAAF at such high thicknesses is usually ≈ 15–33 $m^2\ g^{-1}$ and, generally, more frequently around 20 $m^2\ g^{-1}$ [24], thus, the real surface of PAAFs used is roughly ≈ 50.84 m^2. Field emission scanning electron microscopy (FESEM) micrographs of the top surface, cross section of PAAF and imprint of PAAF on Al surface are shown in Figures 3a–3e**.** The pores on the top surface are non-organized but as these deepen to the Al substrate these become better organized. In H_2SO_4 electrolyte the pore base diameter is usually of the order of a few nm up to around 10 nm [32]. The chemical attack of pore walls by electrolyte widen the pores outward [35]. Due to the long and narrow pores, the large anions of the dye can be most likely adsorbed mainly on the top surface and on the pore wall surface up to some depth they can penetrate. Long anodizing t was thus employed, so the pores become wider enough on the top surface. Therefore, the bulky anions could enter the pores possibly up to a significant depth.

After anodizing, the compact oxide in PAAF embodies small amounts of H_2O, as OH^- and H^+ bound with Al^{3+} and O^{2-} ions or molar H_2O [36], and electrolyte anions [37]. Also, O^-, O, O_2 and O_3 species formed during anodizing [38] may remain, all or some of which being active for dye discoloration. The specimens of Al carrying PAAF were heated at 300 °C for 3 h where these species are expected to be removed or transformed to O^{2-}, except for the electrolyte anions that remain intact. Thus, the adsorptive material is an oxide with electrolyte anions embodied in small amounts. Their presence is expected to affect only faintly the adsorption of dye due to their low concentration [37], and their affinity to sulfonic groups in the dye anion. Then, the Al/oxide specimens were allowed to cool in a desiccator.

The four Al/oxide specimens with total S_g = 74.2 cm^2 were inserted suitably into 50 mL of the original dye solution at 25 °C. Up to t = 2 h the adsorption of dye proceeded negligibly, which shows that the adsorption is generally slow. At 3 × 24 h a percentage of ≈ 65% of dye was removed, at 4 × 24 h this percentage was ≈ 76% while at 5 × 24 h it was ≈ 78%, thus after 4 × 24 h the uptake of dye proceeded only slightly. Despite the long time 5 × 24 h of contact of oxide with dye solution and the small volume of solution, the dye was not totally removed. The initial 50 mL dye solution contains 1.701×10^{-6} mol or 1.0242×10^{18} molecules. Adopting a surface for each molecule 8.83×10^{-18} m^2 [2] and a densely packed monolayer of adsorbed dye molecules, the occupied surface is ≈ 7.05 m^2 << 50.84 m^2. The adsorption is thus slow, while just a small part of the real oxide surface can be occupied by the dye taken up if a monolayer were formed. These results are explained in the following.

The large molecule/anion of dye has a complex structure embracing aromatic amines, heterocyclic azo-aromatic rings, chromophore groups, phenolic-hydrogen atoms, amino-hydrogen atoms, Cl substituents in azo-aromatic and sulfonic groups in aromatic rings. Each of them exhibits a specific adsorption behavior on oxide surface. The surface of oxide has strong adsorptive Lewis acidic sites Al^{3+} and basic sites O^{2-} [24-26]. Some basic (or nucleophile) and/or acidic (or electrophile) sites of dye anion can, accordingly, be attached on them.

Separate species which may stick on oxide surface are (up to 6) $-SO_3^-$ on Al^{3+} acidic sites, (up to 2) detached phenolic acidic H^+ on O^{2-} basic surface sites and parallel (up to 2) $-O^-$ of phenolic –OH on Al^{3+} sites, (up to 14) N atoms with unpaired electrons on Al^{3+} sites, (up to 4) amino-hydrogens HN< on O^{2-} surface sites and (up to 18) benzene hydrogens HAr. Due to the stability of benzene rings and strong bond H–Ar (stronger than H–R, e.g., in terms of bond decomposition enthalpy [39]), the H–Ar hydrogens are not prone to adsorb. But, due to the partially delocalized p orbital electrons in π bonds of seven benzene rings and of the two heterocyclic rings embracing C and N atoms, these rings must show Lewis basic behavior. Also, in the heterocyclic rings and in the two –N=N– groups connected with benzene rings, the solitary sp^2 electron pairs in N atoms assign to them a basic (or nucleophilic) behavior.

If, hypothetically, all these species were properly oriented and arranged in a plane parallel to the surface, the adsorption behavior of an anion would be about the summed contributions of the separate species. However, the molar geometry is complex stereoscopic and only a few of those species can concurrently approach the surface and at proper orientation for adsorption. Hence, the adsorption may vary from weak reversible physical to strong irreversible chemical, depending on the orientation of dye molecule/anion with respect to the surface, the number of species stuck and the bonding strength. The above justifies a relatively slow rate of dye adsorption.

How to cite this article: Patermarakis G, Vassiliadis AA. Mechanism of C.I. Reactive Red 120 Uptake from Solution by Anodic Alumina Films. Curr Trends Fashion Technol Textile Eng. 2023; 8(3): 555737. DOI: 10.19080/CTFTTE.2023.08.555737

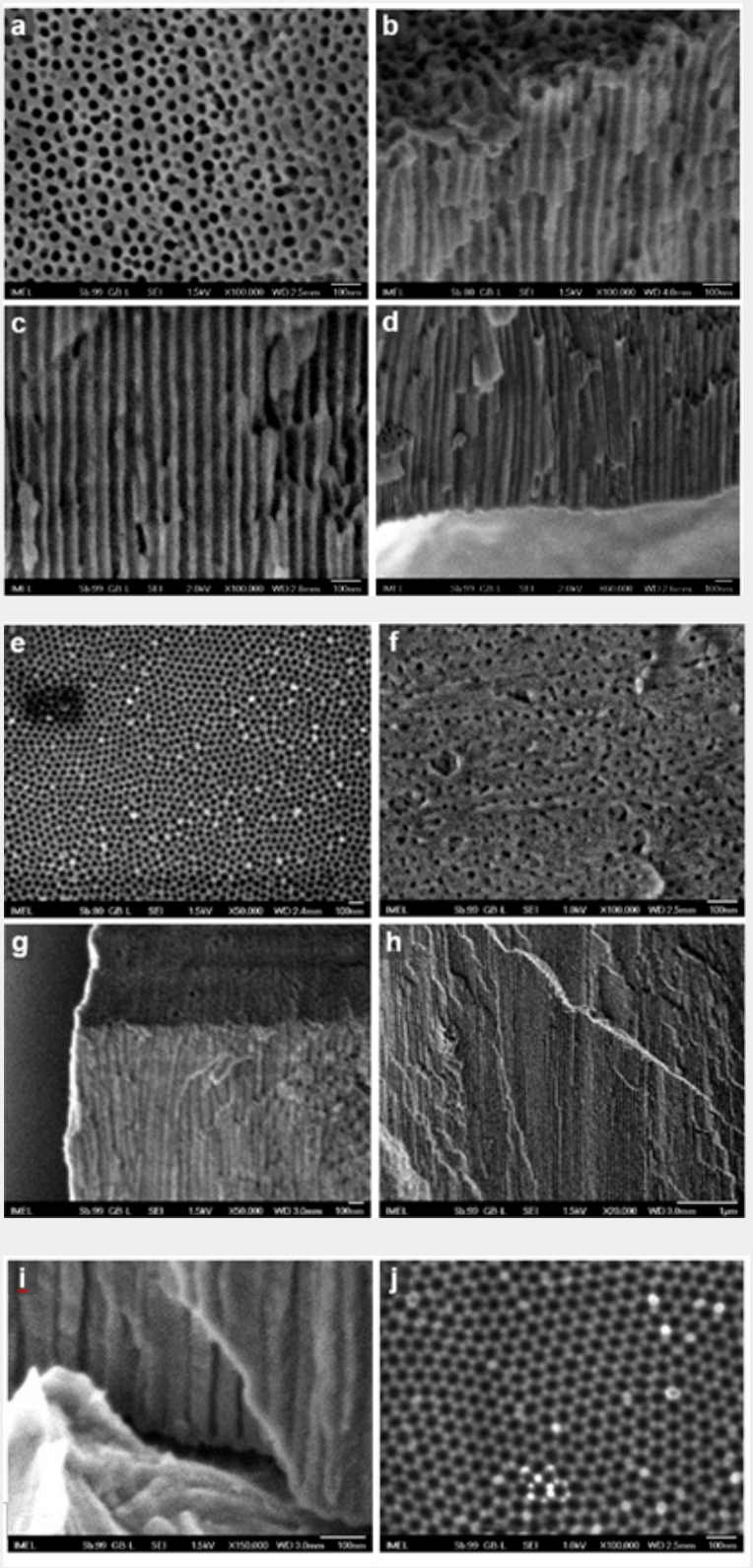

Figure 3: FESEM micrographs of PAAF formed at 7200 s (a), (b), (c), (d), (e) and at 2280 s (f), (g), (h), (i), (j) where the outer surface (a), (f), the outer layer with both the cross section and outer surface (b), (g), the cross section at the middle of film thickness (c), (h), the cross section above the Al substrate (d), (i) and the imprint of PAAF on Al (e), (j) are shown.

How to cite this article: Patermarakis G, Vassiliadis AA. Mechanism of C.I. Reactive Red 120 Uptake from Solution by Anodic Alumina Films. Curr Trends Fashion Technol Textile Eng. 2023; 8(3): 555737. DOI: 10.19080/CTFTTE.2023.08.555737

Up to the time 5 × 24 h an almost limiting amount of adsorbed dye is reached, then the adsorption progress becomes very slow or almost stops. As already noted in PAAF the pore base diameter is of the order of up to about 10 nm [32]. The surface density of pores at the conditions employed is of the order of 10^{10} cm^{-2} [35]. The dye anions are large and difficult to penetrate deep into the pores and be adsorbed at pore bases too. Their adsorption is favored mostly on the top film surface and in the pore walls of an outer film layer. Such large and complex molecules with complex adsorption mechanisms may also favor an adsorption exceedingly locally a monolayer. Gradually, the adsorbed species block the pores from the mouths up to some depth, hindering further adsorption. The uptake of dye on the top surface may be reversible, proceeding up to a quasi-equilibrium limit. But the bulky molecules that enter deeper into the pores are entrapped. Their desorption from the pore walls and egress from pores is difficult or even unfeasible. Also, the pore walls of oxide are hydrated, relatively slowly at ambient temperature, to a swelled hydrated oxide [36], delaying or even stopping the adsorption. This hydration further restricts the mobility of dye anions adsorbed on the inner walls of pores.

After the experiment, the Al/oxide specimens carrying the dye (Al/oxide/dye specimens) were dried in air stream. Figure 4a shows the photograph of the surface of one of thus dried Al/oxide/dye specimen. By bending up to an angle ≈ 90° and resetting one of them, the dye layer remained adhered on the surface. An Al/oxide/dye specimen was additionally left to further dry in a desiccator at ambient temperature for 1 week. It was then bent around the vertical axis of symmetry of anodized Al specimen surface up to ≈ 90° for one only time and restored. A dry multimolecular layer dye was detached in the form of flakes and a surface region, mainly around the axis, was revealed with negligible remaining adsorbed dye (Figure 4b). In this region, the oxide remained strongly adhered on the Al surface and only the dye was removed. Hence, the pore wall surface contributes trivially to dye uptake. A first layer must be physically and chemically adsorbed on the accessible surface. Then, the dye is accumulated almost solely on the top surface.

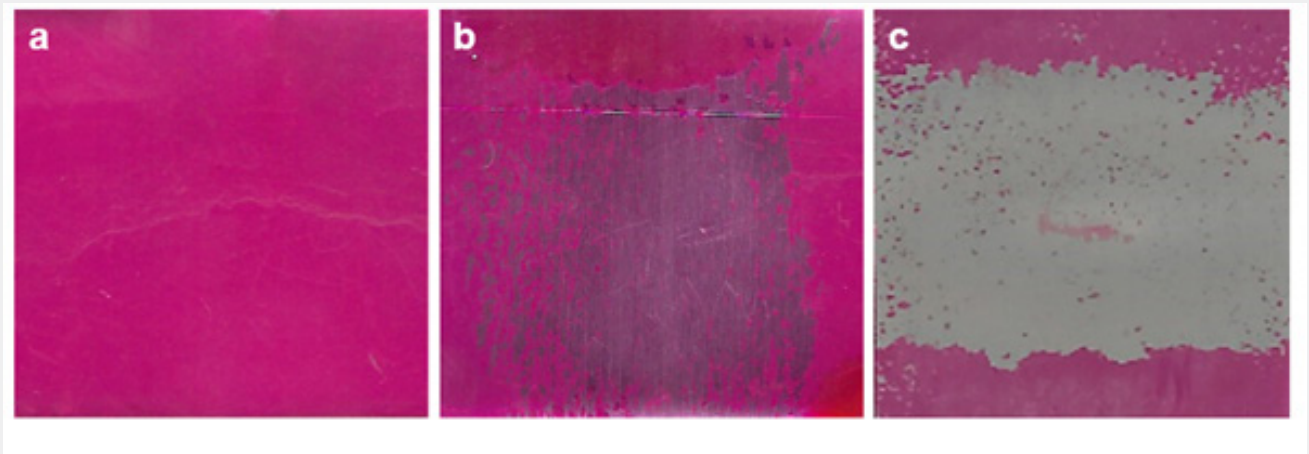

Figure 4: The surface of Al/oxide specimen 3 × 3 cm^2 with taken up RR 120 (a). Similar surfaces after the Al/oxide/dye specimens were bent up to about 90° and restored where the detachment of dry dye layer from the surface is distinguished (b), (c). PAAFs were formed at 7200 s (a), (b) and 2280 s (c).

The dye avails many species able to interact and bind physically or chemically to oxide surface. After an about monomolecular layer is adsorbed, then dimerization/aggregation and/or flocculation/coagulation of the dye mainly on the top surface must occur resulting finally in the formation of the multimolecular dye layer on it. The hues of dye in solution and of the dye in Al/oxide/dye specimen wet and dried in both air stream and desiccator were identical. If dimerization/aggregation occurred, some bonds would be broken and new would be formed. The sensitive chromophore groups –N=N– would be also affected and most probably broken to some extent. No discernible change of coloration was observed; so, even if occurring, dimerization/aggregation is negligible. It seems that the dye is accumulated in a multimolecular layer in the top surface of PAAF by flocculation/coagulation. Indeed, the molecule/anion of dye is large enough and charged, thus it can behave as a micelle. The removal of H_2O

How to cite this article: Patermarakis G, Vassiliadis AA. Mechanism of C.I. Reactive Red 120 Uptake from Solution by Anodic Alumina Films. Curr Trends Fashion Technol Textile Eng. 2023; 8(3): 555737. DOI: 10.19080/CTFTTE.2023.08.555737

from the system Al/oxide/dye in desiccator reduces or eliminates the hydrogen bonding, dipole–dipole bonds, or van der Waals forces. The physical/chemical adsorption bonds weaken, then a multilayer of dye molecules is easily detached by just bending the Al specimen.

The final pH of solution was 7.15; its rise is explained as follows. The charge of dye anion on alumina surface must be compensated (at least partly) by the charge of H^+ ions that stick on the adjacent O^{2-} or on contaminant SO_4^{2-} ions in surface lattice sites. For the system oxide + H_2O, H^+ and OH^- are also attached on O^{2-} and Al^{3+} sites by the dissociative adsorption of H_2O. Then, H_2O molecules can also be chemically or physically adsorbed on the surface which carries OH^- and unsaturated Al^{3+} and O^{2-} sites [36]. As before noted, the adsorption of dye anion involves mostly Al^{3+} surface sites. So, during the progress of adsorption the portion of Al^{3+} sites occupied increases. Concurrently the dissociative adsorption of H_2O produces H^+ ions that are bound mostly to O^{2-} sites and secondarily to contaminant SO_4^{2-} sites, while part of OH^- ions are bound to free Al^{3+} sites and the rest pass into the solution. During the concurrent competitive adsorption of dye anions and dissociative H_2O adsorption the pH rises. While pH rise is mainly due to dye adsorption occurring in the initial stage of experiment, the prolonged flocculation/coagulation may also exert some effect on it. The detailed mechanism of flocculation/coagulation and its effect on pH are beyond the scope of this study.

To check further the previous dye uptake result, four PAAFs were also formed at the same conditions but at t = 2280 s, each exhibiting m = 0.1567 g, $h_f \approx 32.2$ μm [35] and smaller average pore diameter in top surface (Figure 3f) and across the PAAF (Figures 3g–3i). They were also heated at 300 °C for 3 h, allowed to cool in a desiccator and inserted in a similar dye solution. After 3 × 24 h, 4 × 24 h and 5 × 24 h the removal of dye was proceeded by ≈ 58%, 70% and 71%, respectively. Then, the Al/oxide/dye specimens were dried in air stream. As previously, after bending and resetting one of them, the dye layer remained adhered on the surface. Another specimen remained in a desiccator for 1 week.

Figure 4c presents the photograph of the surface of Al/oxide/dye specimen after its bending at an angle up to ≈ 90°, now around the horizontal axis, and resetting. It appears that the dye does not remain adsorbed on the surface of pore walls and after desiccation the multimolecular layer on top surface is almost totally removed/exfoliated. This, together with the previous results, shows that the dye is removed by bending the specimen around any axis. After the mixed physical and chemical adsorption of the first about monomolecular dye layer, its further addition on the top surface of oxide must take place by almost only flocculation/coagulation occurring above the first adsorbed layer. Their initiation is catalyzed by this layer formed initially on the solid surface. Then, the flocculation/coagulation processes, taking place among the surface of dye layer and dye molecules/anions (micelles) in solution, proceed by themselves. As the concentration of micelles in solution decreases with time, the rate of dye uptake similarly falls.

The detailed mechanism and kinetics of dye uptake may change with temperature. The disclosure of its precise mechanism and kinetics exceeds the scope of this work, that is a first approach to dye uptake mechanism. The amount of adsorbed dye must increase mainly with S_g and much less with the surface density, length, base diameter and mean diameter of pores for the PAAFs used. PAAFs formed in other electrolytes (e.g., H_3PO_4) give wider pores but smaller surface pore density [29-32]. For a given S_g, the adsorption on the pore walls of each pore is enhanced, but the decrease in the surface density of pores reduces in turn the amount of dye absorbed on pore walls. Due to slow adsorption and its occurrence almost solely on the top surface of PAAF and around pore mouths, the change in PAAF structure is expected to affect relatively weakly the specific adsorption rate (mol s^{-1} m^{-2}). The second experiment of dye uptake showed that the use of non-porous film may be equally effective, possibly above some limiting film thickness.

After drying the system Al/oxide/multimolecular dye layer by several methods (e.g., desiccation, vacuum, gentle heating by different ways), the dry dye is readily mechanically removed, and the surface is thus renewed. This method may be optimized from many points of view, regarding the physicochemical properties of the surface of non-porous anodic film, the conditions chosen for faster adsorption and flocculation/coagulation and final dye uptake efficiency, as well as the techniques and conditions for both drying and mechanical removal of the dried dye. Use of a resistant elastic support on which an alumina film has been firmly deposited can allow the easy removal of dye. After successive deformations and restorations of support, or vibrations, or mechanical impacts, C.I. Reactive Red 120 will be completely removed. In addition, this method is fully environmentally friendly.

Conclusion

The initial stage of RR 120 uptake by the surface of PAAFs is a mixed physical and chemical adsorption process, in which many different basic (nucleophile) and acidic (electrophile) species of the large dye anion are involved that can be adsorbed on Lewis basic and acidic sites of the oxide surface. It is a slow enough process despite the fact that this surface is a highly adsorptive and active one. Adsorption of RR 120 on the mesopores of the oxide used occurs almost exclusively at the top surface and around

How to cite this article: Patermarakis G, Vassiliadis AA. Mechanism of C.I. Reactive Red 120 Uptake from Solution by Anodic Alumina Films. Curr Trends Fashion Technol Textile Eng. 2023; 8(3): 555737. DOI: 10.19080/CTFTTE.2023.08.555737

pore mouths. After a mixed physical–chemical adsorption of an about monomolecular layer on the surface, a multilayer grows by combined molecular forces among dye anions and water, thus, adsorption is followed by flocculation/coagulation. After removing H_2O from this layer (i.e., reduction or elimination of hydrogen bonding and molecular forces, such as dipole–ion, dipole–dipole), it is easily exfoliated from the surface and a recovery of separated PAAF and dye is then possible. These results predict many ways to improve the whole method from many points of view as regards the rate of dye uptake, the final amount of dye taken up and the ease of separation of dry dye from adsorbent. The method can be improved to result in an almost complete removal of dye from solution.

References

1. Georgiou D, Kalis M, Patermarakis G, Vassiliadis AA (2017) Destruction of azo-reactive dyes by ozonation and the synergetic effect of a radio-frequency alternating electric field inductance device. Curr Trends Fashion Technol Textile Eng 1(2): 42-47.
2. Santos DC, Adebayo MA, Pereira SFP, Prola LDT, Cataluña R, et al. (2014) New carbon composite adsorbents for the removal of textile dyes from aqueous solutions: Kinetic, equilibrium, and thermodynamic studies. Korean J Chem Eng 31(8): 1470-1479.
3. Çelekli A, Al-Nusimi AI, Bozkurt H (2019) Adsorption kinetic and isotherms of Reactive Red 120 on Moringa oleifera seed as an eco-friendly process. J Mol Struct 1195: 168-178.
4. Harrelkas F, Azizi A, Yaacoubi A, Benhammou A, Pons MN (2009) Treatment of textile dye effluents using coagulation-flocculation coupled with membrane processes or adsorption on powdered activated carbon. Desalination 235(1-3): 330-339.
5. Georgiou D, Aivasidis A (2012) Cotton-textile wastewater management: investigating different treatment methods. Water Environ Res 84(1): 54-64.
6. Sarayu K, Sandhya S (2012) Current technologies for biological treatment of textile wastewater-A review. Appl Biochem Biotechn 167(3): 645-661.
7. Gupta VK, Khamparia S, Tyagi I, Jaspal D, Malviya A (2015) Decolorization of mixture of dyes: A critical review. Glob J Environ Sci Manage 1(1): 71-94.
8. Roulia M, Vassiliadis AA (2009) Clay-catalyzed phenomena of cationic-dye aggregation and hydroxo-chromium oligomerization. Micropor Mesopor Mater 122(1-3): 13-19.
9. Roulia M, Vassiliadis AA (2008) Sorption characterization of a cationic dye retained by clays and perlite. Micropor Mesopor Mater 116(1-3): 732-740.
10. Georgiou D, Melidis P, Aivasidis A, Gimouhopoulos K (2002) Degradation of azo reactive dyes by UV radiation in the presence of hydrogen peroxide. Dyes Pigments 52(2): 69-78.
11. Soares PA, Silva TFCV, Manenti DR, Souza SMAGU, Boaventura RAR, et al. (2014) Insights into real cotton-textile dyeing wastewater treatment using solar advanced oxidation processes. Environ Sci Pollut Res Int 21(2): 932–945.
12. Asghar A, Raman AAA, Daud WMAW (2015) Advanced oxidation processes for in-situ production of hydrogen peroxide/hydroxyl radical for textile wastewater treatment: a review. J Clean Prod 87: 826-838.
13. Cardoso JC, Bessegato GG, Zanoni MVB (2016) Efficiency comparison of ozonation, photolysis, photocatalysis and photoelectrocatalysis methods in real textile wastewater decolorization. Water Res 98: 39-46.
14. Cui M, Jang M, Cho SH, Elena D, Khim J (2011) Enhancement in mineralization of a number of natural refractory organic compounds by the combined process of sonolysis and ozonolysis (US/O_3). Ultrason Sonochem 18(3): 773-780.
15. Sathishkumar P, Mangalaraja RV, Anandan S (2016) Review on the recent improvements in sonochemical and combined sonochemical oxidation processes - A powerful tool for destruction of environmental contaminants. Renew Sust Energ Rev 55: 426-454.
16. Babu SG, Ashokkumar M, Neppolian B (2016) The role of ultrasound on advanced oxidation processes. Top Curr Chem (Z) 374(5):75.
17. Sugiarto AT, Ito S, Ohshima T, Sato M, Skalny JD (2003) Oxidative decoloration of dyes by pulsed discharge plasma in water. J Electrostat 58: 135-145.
18. Zhang L, Sun B, Zhu X (2009) Organic dye removal from aqueous solution by pulsed discharge on the pinhole. J Electrostat 67: 62-66.
19. Jiang B, Zheng J, Qiu S, Wu M, Zhang Q, Yan Z, Xue Q (2014) Review on electrical discharge plasma technology for wastewater remediation. Chem Eng J 236: 348-368.
20. Koutahzadeha N, Esfahania MR, Arcea PE (2016) Removal of Acid Black 1 from water by the pulsed corona discharge advanced oxidation method. J Water Process Eng 10: 1-8.
21. Shah AR, Tahir H (2019) Optimization of sono-electrocoagulation process for the removal of dye using central composite design. Mehran University Research Journal of Engineering & Technology 38(2): 399-414.
22. Patermarakis G, Fountoukidis E (1990) Disinfection of water by electrochemical treatment. Water Res 24: 1491-1496.
23. Neta P (1972) Reactions of hydrogen atoms in aqueous solutions. Chem Rev 72(5): 533-543.
24. Patermarakis G, Pavlidou C (1994) Catalysis over porous anodic alumina catalysts. J Catal 147: 140-155.
25. Patermarakis G, Nicolopoulos N (1999) Catalysis over porous anodic alumina film catalysts with different pore surface concentrations. J Catal 187: 311-320.
26. Patermarakis G, Moussoutzanis K, Chandrinos J (1999) Preparation of ultra - active alumina of designed porous structure by successive hydrothermal and thermal treatments of porous anodic Al_2O_3 films, Appl Catal A: General 180: 345-358.
27. Ganley JC, Riechmann KL, Seebauer EG, Masel RI (2004) Porous anodic alumina optimized as a catalyst support for microreactors. J Catal 227(1): 26-32.
28. Lee W, Park SJ (2014) Porous anodic aluminum oxide: anodization and templated synthesis of functional nanostructures. Chem Rev 114(15): 7487-7556.
29. Keller F, Hunter MS, Robinson DL (1953) Structural features of oxide coatings on aluminum. J Electrochem Soc 100(9): 411-419.
30. Young L (1961) Anodic oxide films, Academic Press, London.
31. Diggle JW, Downie TC, Goulding CW (1969) Anodic oxide films on aluminum. Chem Rev 69(3): 365-405.

How to cite this article: Patermarakis G, Vassiliadis AA. Mechanism of C.I. Reactive Red 120 Uptake from Solution by Anodic Alumina Films. Curr Trends Fashion Technol Textile Eng. 2023; 8(3): 555737. DOI: 10.19080/CTFTTE.2023.08.555737

32. Patermarakis G, Moussoutzanis K (2011) Transformation of porous structure of anodic alumina films formed during galvanostatic anodising of aluminium. J Electroanal Chem 659(2): 176-190.

33. The Colour Index™, colour-index.com published online by The Society of Dyers and Colourists and American Association of Textile Chemists and Colorists.

34. Dobos D (1975) Electrochemical data: A handbook for electrochemists in industry and universities, Elsevier.

35. Patermarakis G, Triantis TM (2019) Transformation of porous nanostructure and self-ordering of anodic alumina films during potentiostatic anodising of aluminium. Curr Top Electrochem 21: 21-39.

36. Patermarakis G, Kerassovitou P (1992) Study on the mechanism of oxide hydration and oxide pore closure during hydrothermal treatment of porous anodic Al_2O_3 films. Electrochim Acta 37: 125-137.

37. Thompson GE, Furneaux RC, Wood GC (1978) Electron microscopy of ion beam thinned porous anodic films formed on aluminium. Corros Sci 18: 481-498.

38. Patermarakis G (2021) A novel theory on the mechanisms of generation, transport and release of oxygen gas and electronic current in anodic alumina film during Al anodizing. Curr Top Electrochem 23: 97-115.

39. Atkins P (2010) Physical chemistry, Oxford University Press.

This work is licensed under Creative Commons Attribution 4.0 Licens
DOI: 10.19080/CTFTTE.2023.08.555737

Your next submission with Juniper Publishers will reach you the below assets

- Quality Editorial service
- Swift Peer Review
- Reprints availability
- E-prints Service
- Manuscript Podcast for convenient understanding
- Global attai nment for your research
- Manuscript accessibility in different formats

(Pdf, E-pub, Full Text, Audio)

- Unceasing customer service

Track the below URL for one-step submission
https://juniperpublishers.com/online-submission.php

How to cite this article: Patermarakis G, Vassiliadis AA. Mechanism of C.I. Reactive Red 120 Uptake from Solution by Anodic Alumina Films. Curr Trends Fashion Technol Textile Eng. 2023; 8(3): 555737. DOI: 10.19080/CTFTTE.2023.08.555737